Published in "Molecular Cancer Therapeutics
doi:10.1158/1535-7163.MCT-10-0666 , 2011"
which should be cited to refer to this work.

# Everolimus augments the effects of Sorafenib in a syngeneic orthotopic model of hepatocellular carcinoma

Anne-Christine Piguet[1], Bettina Saar[2], Ruslan Hlushchuk[3], Marie V. St-Pierre[1], Paul MJ McSheehy[4], Vesna Radojevic[1], Maresa Afthinos[1], Luigi Terracciano[5], Valentin Djonov[3], Jean-François Dufour[1, 6]

[1]*Hepatology, Department of Clinical Research, University of Berne, Berne, Switzerland*

[2] *Institute for Diagnostic Radiology, Inselspital Berne, Berne, Switzerland*

[3] *Institute of Anatomy, University of Fribourg, Fribourg, Switzerland*

[4] *Novartis Institutes for Biomedical Research, Oncology Research, Basel, Switzerland*

[5]*Institute of Pathology, University Hospital, Basel, Switzerland*

[6]*University Clinic of Visceral Surgery and Medicine, Inselspital Berne, Berne, Switzerland*

**Running title:** Sorafenib and everolimus in HCC

**Key words:** sorafenib, everolimus, hepatocellular carcinoma, mTOR, intussusception, vessel sprouting, angiogenesis, targeted therapy

**Abbreviations:** ACI, American cancer institute; EC, endothelial cells; HCC, hepatocellular carcinoma; MH, Morris hepatoma; HHSEC, Human hepatic sinusoidal endothelial cells.

**Notes:**

**Financial support:** This work was supported by the Bernische Krebsliga, Oncosuisse, The Swiss National Foundation, The Hassan Badawi Foundation and an unrestricted grant from Novartis (all to JFD).

**Corresponding authors:** Bettina Saar
Institute of Radiology
University of Berne
Murtenstrasse 35
CH-3010 Berne
Switzerland
Tel: + 41 31 632 31 91
Fax: + 41 31 632 49 97
E-mail: bettina.saar@insel.ch

**Potential conflict of interest:** Paul MJ McSheehy is a Novartis' employee.

**Words count and total number of figures and table**

Words in abstract: 250

Words in body of the manuscript: 4181

References: 32

Figures: 6

Tables: 0

Supplementary figures: 4

**ABSTRACT**

Sorafenib targets the Raf/mitogen activated protein kinase, VEGF and PDGF pathways and prolongs survival patients in advanced hepatocellular carcinoma (HCC). Everolimus inhibits the mammalian target of rapamycin, a kinase overactive in HCC. To investigate whether the antitumor effects of these agents are additive, we compared a combined and sequential treatment regimen of everolimus and sorafenib with monotherapy. After hepatic implantation of Morris Hepatoma cells, rats were randomly allocated to everolimus (5mg/kg, 2x/week), sorafenib (7.5mg/kg/day), combined everolimus and sorafenib, sequential sorafenib (2 weeks) then everolimus (3 weeks), or control groups. Magnetic resonance imaging quantified tumor volumes. Erk1/2, 4E-BP1 and their phosphorylated forms were quantified by immunoblotting. Angiogenesis was assessed *in vitro* by aortic ring and tube formation assays, and *in vivo* with Vegf-a mRNA and vascular casts. After 35 days, tumor volumes were reduced by 60%, 85% and 55%, relative to controls, in everolimus, the combination and sequential groups, respectively ($p<0.01$). Survival was longest in the combination group ($p<0.001$). Phosphorylation of 4E-BP1 and Erk1/2 decreased after everolimus and sorafenib, respectively. Angiogenesis decreased after all treatments ($p<0.05$), although sorafenib increased Vegf-a mRNA in liver tumors. Vessel sprouting was abundant in control tumors, lower after sorafenib and absent after the combination. Intussusceptive angiogenic transluminal pillars failed to coalesce after the combination. Combined treatment with everolimus and sorafenib exerts a stronger antitumoral effect on MH tumors than monotherapy. Everolimus retains antitumoral properties when administered sequentially after sorafenib. This supports the clinical use of everolimus in HCC, both in combination with sorafenib or after sorafenib.

## INTRODUCTION

Sorafenib is the only drug for which randomized control trials have shown an improved survival in advanced hepatocellular carcinoma (HCC) [1], [2], and is the only systemic targeted therapy approved for clinical use in many countries. Sorafenib inhibits the kinase activity of Raf, an enzyme operative within the mitogen-activated protein kinase (MAPK) signaling pathway and inhibits the vascular endothelial growth factor receptors (VEGFR) and platelet-derived growth factor receptor-β (PDGF-β). In many cases of HCC, Ras kinase is over-expressed or mutated and the Raf/MAPK pathway is activated [3]. As a result of the inhibition of these target molecules, sorafenib decreases tumor microvessel density and exerts an anti-proliferative effect on tumor cells [4]. Despite these actions, sorafenib only extends the life expectancy of patients with HCC by a few months, suggesting that other signaling pathways remain active.

Additional pathways implicated in tumorigenesis include those signaling through PI(3)K/Akt/mTOR, WNT/β-catenin, insulin-like growth factor, hepatocyte growth factor/c-MET and growth factor-regulated angiogenic signaling (VEGF, PDGF, EGF) [5]. In this study we focused on the PI(3)K/Akt/mTOR signaling cascade. The mammalian target of rapamycin (mTOR), which is the downstream target of the serine/threonine kinase Akt, increases protein synthesis and cell proliferation in response to growth factors. Pharmacological inhibition of mTOR by rapamycin and its analogues arrests the cell cycle by abrogating the PI(3)K/Akt-mediated proliferative signals. Moreover, mTOR inhibitors reduce the expression of VEGF, which is associated with tumor angiogenesis [6]. We reported previously that inhibition of mTOR significantly slows tumor growth, impairs the tumor angiogenesis that occurs by sprouting, and improves survival in an experimental HCC model [6]. Everolimus, a rapamycin analogue, is the only mTOR inhibitor currently under

investigation in clinical HCC trials, either as monotherapy or combined with other therapeutic options, such as bevacizumab, sorafenib, and transarterial chemoembolization with doxorubicin. Since the activities of mTOR inhibitors and sorafenib occur at separate stages along two signaling pathways, their combination could be complementary and provide more effective suppression of HCC. Although the combination of sorafenib and rapamycin has shown synergistic inhibition of HCC xenografts [7], important information is lacking with respect to the mechanisms of this synergism and the specific effects of the drug combination on angiogenic processes. Additional uncertainties relate to the most effective means of administering the drug combination and whether patients who have been unresponsive or intolerant to sorafenib could subsequently benefit from an mTOR inhibitor.

We asked whether the anti-proliferative and anti-angiogenic properties of everolimus and sorafenib in liver tumors are additive when administered in combination, whether their concomitant use improves survival, and whether administration of everolimus sequentially after sorafenib is beneficial. We chose an orthotopic syngeneic rat model of HCC and examined the effects of everolimus and sorafenib on tumor vasculature and different cell types. Our results provide a rationale for combining everolimus with sorafenib in HCC.

## MATERIAL AND METHODS

### Animals and surgical procedures

Animal experiments were approved by the Local Animal Use Committee. The livers of male ACI rats (Harlan, Indianapolis, IN), 10-12 weeks old, were surgically implanted with tumors derived from Morris Hepatoma MH-3924A cells as previously described [6], [8].

### Animal treatment protocol

On day 6 post tumor implantation, the rats were randomized to a group receiving either everolimus (5mg/kg 2x/week; Novartis, Basel, Switzerland; structural formula in Supplementary Figure 1A), sorafenib (7.5mg/kg/day; Bayer HealthCare Pharmaceuticals Montville, NJ; structural formula in Supplementary Figure 1B), the combination of everolimus and sorafenib, or the successive treatment of sorafenib for 2 weeks followed by everolimus for 3 weeks, or to a control group. Drugs and vehicle were administered by gavage. Rats were euthanized on day 42 after tumor implantation. In a second series of experiments designed to measure survival, animals were treated until the appearance of signs of wasting or suffering that indicated distress (deterioration of the general state of the animals, loss of weight greater than 20%, severe piloerection, harderian gland secretion, abnormal posture and behaviour), at which point they were euthanized. The investigators were blinded to treatment allocation.

### MR Imaging

Liver MR imaging with a commercial 3.0 Tesla system (TIM TRIO, Siemens, Erlangen, Germany) of tumors was first performed on day 11 after tumor implantation and weekly thereafter. All animals received food and water ad libitum. Animals were anesthetized and placed prone and head first in an eight-channel-wrist coil. After visualization of the liver, a

volume adapted high resolution T2 weighted Turbo Spin Echo sequence with fat suppression was acquired in the coronal plane and repeated in the axial acquisition direction (repetition time/echo time max/66; voxel size 0.3 x 0.3 x 2 $mm^3$, matrix 384, turbo factor 14, acquisition time 4.48 min). Data were analyzed on a post-processing workstation (Leonardo, Siemens, Erlangen, Germany). The largest diameter of the tumor was measured in three planes perpendicular to each other. The volume of tumor ellipsoids in $mm^3$ was calculated as: $4/3 \cdot \pi \cdot r_1 \cdot r_2 \cdot r_3$ (with $r_1$, $r_2$ and $r_3$ representing perpendicular radii of the lesion).

**Immunohistochemistry**

Tumor necrosis was assessed by staining tumor sections with Giemsa and by quantifying the necrotic area using the software Metamorph. Tumoral apoptosis was measured in paraffin-embedded sections by cleaved-caspase 3 immunostaining (Cell Signaling, Beverly, MA). Tumoral hypoxia was measured in paraffin-embedded sections by HIF-1α immunostaining (Abcam, Cambridge, UK) with classification as follows: 0, no HIF positive tumoral cells; 1, <10% HIF positive tumoral cells; 2, 10-20% HIF positive tumoral cells; 3, 20-50% HIF positive tumoral cells; 4, >50% HIF positive tumoral cells. Tumoral invasiveness was assessed in paraffin-embedded sections by immunohistochemical staining for E-Cadherin (Abcam).

**Real time quantitative PCR**

Total RNA was extracted from liver by means of an RNeasy Mini Kit (Qiagen, Hombrechtikon, Switzerland) then was reverse-transcribed using SuperscriptIII Reverse Transcriptase (Invitrogen, Basel, Switzerland) and a random hexamer mix. The probe and primers for *Vegf-a* were obtained from TaqMan® Gene Expression Assays (Applied Biosystem, Rotkreuz, Switzerland) and quantitative PCR was performed using an ABI

PRISM 7500 Sequence Detection System and the TaqMan universal PCR Master Mix, according to standard protocols. The $C_t$ for each gene were standardized against ribosomal RNA (18s) to obtain the $\Delta C_t$ values. The $\Delta\Delta C_t$ values were calculated by substracting the $\Delta C_t$ values of animals treated with vehicle from $\Delta C_t$ values of rats treated with the different drugs. Relative fold increases or decreases were calculated using the formula $2^{-\Delta\Delta Ct}$. All reactions were performed in triplicate.

**Vascular casting**

As previously described [9], the liver vasculature was perfused with a freshly prepared solution of Mercox® (Vilene Company, Japan) containing 0.1 ml accelerator per 5 ml resin. One hour after perfusion, the tumors were excised and macerated in 15% potassium hydroxide. After 3 to 4 weeks, the casts were washed and dehydrated in ethanol and desiccated under vacuum. Samples were layered with gold to a thickness of 10 nm and examined in a Philips XL 30 FEG scanning electron microscope.

**Cells and culture conditions**

MH-3924A (Morris Hepatoma, MH) cells were obtained from DKFZ (Heidelberg, Germany) and not further authenticated. Isolated rat aortic endothelial cells (EC) were cultured as described by Semela *et al.* [6] and characterized by immunofluorescence with antibodies to vonWillebrand Factor/Factor VIII and CD31 (P-CAM). Human hepatic sinusoidal endothelial cells (HHSEC) (ScienCell Research Laboratories, San Diego, CA) were characterized by the supplier by immunofluorescence with antibodies to vonWillebrand Factor/Factor VIII and CD31 (P-CAM)

**$^3$H-Thymidine incorporation assay**

MH and rat aortic endothelial cells were serum-starved overnight, then incubated with various concentrations of everolimus and sorafenib for 24 hours. $^{3}$H-Thymidine (0.2 μCi/ml, Amersham Biosciences, Otelfingen, Switzerland) was added in the presence of drugs and the incubation continued for 24 hours. Cell proliferation was measured by counting the incorporation of $^{3}$H-Thymidine. Experiments were repeated 3 times in triplicate.

**Rat aortic ring assay**

Aortic rings were prepared as previously described [6]. Everolimus and/or sorafenib were added 24h after preparation and rings were incubated for 5 days. For sequential drug treatment, rings were incubated with sorafenib for two days, the medium was changed and everolimus was added. At day 5, the rings were fixed and stained according to a Diff-Quick solution II protocol (Diff-Quick Stain Set; Baxter-Dade AG, Switzerland). Vascular outgrowth was quantified by counting the sprouts.

**Tube formation assay**

HHSEC ($4x10^{4}$) were incubated in 24-well plates coated with Matrigel in the presence or absence of everolimus and/or sorafenib. After 72 hours, the area covered with vascular tubes was quantified using the Metamorph software (Molecular Devices, Sunnyvale, CA). Experiments were performed 3 times in duplicate.

**Immunoblot analysis**

Liver tissue was homogenized in RIPA buffer (150 mM NaCl, 1% NP-40, 0.5% Na-deoxycholate, 0.1% SDS and 50 mM Tris-HCl pH 7.4) containing protease and phosphatase inhibitors (Roche, Rotkreuz, Switzerland). Protein concentration was assayed according to Lowry [10]. Equal amount of proteins were separated by SDS-PAGE and transferred to

nitrocellulose membranes, blocked for 1 hour with 5% nonfat milk, then incubated overnight at 4°C with cleaved-Caspase 3, phospho-Erk1/2, phospho-4E-BP1, phospho-Elk1 and phospho-Akt (Ser473) antibodies (Cell Signaling, Beverly, MA). After washing, the membranes were incubated with peroxidase-conjugated secondary antibody (Pierce, Lausanne, Switzerland) and signals were revealed using an enhanced chemiluminescence detection system (Perkin Elmer, Schwerzenbach, Switzerland) and a Fujifilm LAS.100 CCD camera coupled to a computer using the software AIDA 2.1 (Raytest, Urdorf, Switzerland). Membranes were stripped and reincubated with antibodies against total Erk1/2, 4E-BP1, Elk1 and Akt (Cell Signaling). Membranes were stripped again before incubation with anti-β-actin antibody (Sigma-Aldrich Chemie GmbH, Munich, Germany) and protein was normalized for actin expression.

**Statistical analysis**

Data points represent the mean values ± SD. Data were compared by applying the nonparametric Mann-Whitney U test. A p value $<0.05$ was considered statistically significant.

## RESULTS

**Effect of everolimus – sorafenib on tumor progression.** MR imaging 35 days after tumor implantation showed smaller tumors in the treated livers than the untreated livers (Figure 1A). Tumor volumes were significantly smaller in the combined sorafenib + everolimus group than all other groups ($p<0.01$ vs. control; $p<0.05$ vs. sorafenib; $p<0.01$ vs. everolimus and vs. sequential everolimus-sorafenib) (Figure 1B). The sequential sorafenib-everolimus treatment and everolimus monotherapy were equally effective. Monotherapy with sorafenib was the least effective. At harvest, tumor sizes were 166±53 $mm^3$ after combined sorafenib and everolimus, 421±84 $mm^3$ after everolimus, 511±183 $mm^3$ after sorafenib for 2 weeks then everolimus for 3 weeks, 805±317 $mm^3$ after sorafenib, and 1139±238 $mm^3$ for the untreated group. The median survival was longest for the combined everolimus-sorafenib group (70 days, $p<0.001$ vs. control and sorafenib groups), shorter for sorafenib monotherapy (63.5 days) and shortest for the controls (57 days) (Figure 1C). Rats tolerated the treatments for the duration of the study (42 days). The body weights ranged from 234 ±12 g for the combination group to 273 ±14 g for the control group. However, the longer treatment imposed by the design of the survival study was associated with tooth fractures in the rats treated with sorafenib. Tooth fractures were noted after 8 weeks, and could have caused a secondary weight loss. Although the extent of tumor necrosis was not significantly affected by any of the treatments, a higher trend of necrosis was noted in the combined everolimus-sorafenib group (Figure 2A and Supplementary Figure 2A). Treatment with everolimus or sorafenib was associated with apoptosis, more so after sorfanib, as assessed by immunoblots and immunohistochemical detection of cleaved caspase 3 (Figure 2B and 2C). The degree of hypoxia in tumors was estimated by HIF-1α immunostaining. The number of HIF-1α positive tumor cells was higher in the tumors treated with everolimus, sorafenib and the combination than in the control group ($p<0.01$). The number of HIF-1α positive cells was also

significantly greater in the sequential sorafenib-everolimus treated tumors than in controls but achieved a lower statistical score ($p<0.05$) (Figure 2D and Supplementary Figure 2B).

**Antiproliferative and anti-angiogenic effects of everolimus-sorafenib *in vitro*.** Relative to control conditions, the proliferation of rat endothelial cells decreased by 40% in the presence of everolimus (20-200 nM). The effect was not dose dependent and was not potentiated by the addition of sorafenib (Figure 3A). Sorafenib alone from 100 nM to 10 μM had no effect. In contrast, the proliferation of hepatoma MH cells was insensitive to everolimus alone (20-2000 nM). Sorafenib alone was anti-proliferative only at the highest concentration (10 μM). The addition of everolimus lowered the minimal effective concentration of sorafenib to 5 μM (Figure 3B).

The effect of sorafenib and everolimus on angiogenesis *in vitro* was measured in two ways. In the aortic ring assay, everolimus 200 nM and sorafenib 100 nM alone significantly decreased sprouting from aortic rings by 60% (Figure 4A). The combination of drugs, either in a concomitant or sequential regimen, decreased sprouting even further (Figure 4A). In fact, vessel sprouting was most inhibited by the sequential sorafenib-everolimus treatment protocol. The tube formation assay measures the ability of endothelial cells to form a linear structure and in contrast to the ring aortic assay, operates without the confounding influences of pericytes and fibroblasts. Endothelial tube formation was significantly impaired by everolimus both in monotherapy and in combination (Figure 4B). Sorafenib had no effect in this assay.

**Effect of combined everolimus – sorafenib on tumors *in vivo*.** Compared to controls, the mRNA levels of *Vegf-a* were increased by 86% after sorafenib ($p<0.05$) although this effect

was blunted to 49% upon addition of everolimus (Figure 5A). Everolimus alone did not produce a significant effect in *Vegf-a* mRNA. Everolimus alone decreased phosphorylation of 4E-BP1 in total tumor tissue, whereas the addition of sorafenib tended to blunt this effect (Figures 5B and Supplementary Figure 3A). Sorafenib alone decreased the phosphorylation of Erk1/2 in tumors but this effect was lost in combination with everolimus (Figures 5B and Supplementary Figure 3B). Sorafenib alone also decreased the phosphorylation of the Erk1/2 target, Elk1, in tumors (Supplementary Figure 3C and 3D). The phosphorylation of Akt on Ser473, which is a site phosphorylated by the complex mTORC2, was increased in the tumors treated with sorafenib and everolimus (Figure 5C and Supplementary Figure 3E).

Vascular casts revealed abundant sprouting in tumors of the control group, whereas sprouting was reduced in sorafenib treated tumors and absent in tumors treated with everolimus and sorafenib (Figure 6A). Vessels were pierced by pillars in the sorafenib treated tumors as a sign of non-sprouting intussusceptive angiogenesis. In the combination group, pillars were frequent but remained small and were positioned irregularly. Histological analysis of the periphery of the tumor and application of a technique of digital quantification demonstrated that in the combination group, an invasive front intercalated extensively into the surrounding tissue (Figure 6B and Supplementary Figure 4A). In contrast, the periphery of the tumors in the control group was regular and limited by a capsule. The tumor periphery was examined by immunohistochemical staining for expression of E-cadherin. In the tumors cells, E-cadherin was prominent and cytoplasmic regardless of the treatment group. In adjacent non-tumoral hepatocytes at the interface, a peripheral membrane staining of E-cadherin was noted but only in the control group. This feature was not seen in the hepatocytes adjacent to the invading tumor cells in the everolimus+sorafenib group (Supplementary Figure 4B). Despite

the invasive characteristics of the limiting edges of the treated tumors, histological analyses of the lungs of animals from all groups indicated no distant metastases.

**DISCUSSION**

We previously reported that inhibition of the mTOR pathway, which is activated in many cases of HCC [11], [12], [13], decreases VEGF levels, impairs tumor angiogenesis, and results in smaller tumors and longer survival in a rat MH-3924A model of HCC [6]. We now show the benefits of combining an mTOR inhibitor with sorafenib, an inhibitor of B-Raf and Raf-1 kinases, as well as VEGF and PDGF receptor. Our findings show that combined everolimus and sorafenib is a more potent anti-tumor regimen than either agent alone, exerts a stronger anti-angiogenic effect than either agent alone and improves survival in this HCC model. Everolimus also retains its antitumoral potency *in vivo* when administered sequentially after sorafenib, a finding that carries important clinical implications. Our positive results contrast with those of Newell et al., who found no difference in tumor growth with this combination [14]. This disparity is perhaps explained by our propitious choice of an orthotopic syngeneic model, which is a closer representation of HCC than the xenograft model chosen by previous investigators [14], [7] , [15]

HCC is a hypervascular tumor, relying on angiogenesis for growth [16]. Focal hypoxia is a potent angiogenic stimulus and both everolimus and sorafenib treatment regimens exerted their antitumoral effects within a local environment that was subject to such stimuli, as shown by the increased expression of HIF-1α in all treated tumors (Figure 2D). The upregulation of Vegf-a mRNA in the tumor by sorafenib, an effect also reported with other receptor tyrosine kinase inhibitors such as vatalanib [17] and sunitinib [18], can be attributed to a feedback response to the suppressed VEGF receptor signaling [19]. Despite this, hypoxia-driven neovascularisation was not seen in the treated liver tumors. Rather, everolimus and sorafenib impaired angiogenesis and altered the structure of the tumor vascular architecture (Figure 6A). In keeping with our previous findings, where inhibition of mTOR with sirolimus

effected a switch in tumor angiogenesis from sprouting to intussusception [6], the combination of everolimus/sorafenib promoted an increase in the number of vascular pillars but these pillars remained small, which suggests an inability to fuse, and consequently an impairment of the process of intussusception as a means of tumor vascularization. We ascribe the superior ability of the everolimus and sorafenib combination to slow tumor growth to this impaired tumor angiogenesis and vascularization.

The innate resistance of the MH-3924A cells to the anti-proliferative actions of mTOR inhibition and the low sensitivity to Raf/ERK blockade *in vitro* (Figure 3B) did not preclude a response to everolimus and sorafenib when these cells were implanted as solid tumors *in vivo*. Other investigators have reported similar anti-tumoral responses when insensitive cell lines were seeded *in vivo* [20], [21]. The everolimus mediated decrease in proliferation and migration of endothelial cells *in vitro* and impairment of vessel sprouting point to antiangiogenesis as the means by which the resistant tumors became sensitized to mTOR inhibition *in vivo*. Lane *et al*. postulated that the anti-antiogenic effects of everolimus were due to the combination of a reduced VEGF production in tumor cells and direct action on mTOR signalling in non-tumor pericytes and endothelial cells [20]. We have previously reported that another mTOR inhibitor, sirolimus, did decrease VEGF-a in MH-3924A derived tumors under different experimental circumstances [6]. A similar reduction was not detected with everolimus, although the sorafenib-induced increase in VEGF-a mRNA tended to be less acute in the presence of everolimus (Figure 5A). Our findings appear more consistent with inhibition of mTOR signalling in endothelial cells (Figures 3A, 4). The basis for the resistance of MH-3924A cells to everolimus has not been investigated. The presence of an oncogenic mutation in PI-3-kinase catalytic α subunit and PTEN loss of function has been linked to mTOR inhibitor sensitivity [22]. Conversely, selected K-Ras mutations have been linked to

mTOR inhibitor insensitivity, as has overexpression of the myc oncogene [23]. The MH-3924A cells likely overexpress K-Ras since gene amplification was detected in several Morris Hepatoma cell lines [24] but a more extensive genotyping is required to fully explain the response to mTOR signalling inhibition. Genotyping may also explain the basis for the low sensitivity of MH-3924A cells to sorafenib (Figure 3B). Tumor cell lines containing an activating receptor tyrosine kinase mutation are more sensitive to sorafenib whereas cell lines in which multiple signalling pathways drive growth are less sensitive [25]. The growth-inhibitory response of MH-3924A tumors to sorafenib alone was poor (Figure 1B) despite a 50% reduction in ERK phosphorylation (Figures 5B and S3), therefore multiple signalling pathways are likely important for proliferation of MH-3924A cells. Sorafenib can also exert anti-tumor actions independent from the MEK/ERK pathway. Sorafenib is apopotic in tumor tissue (Figures 2B and 2C), an effect likely explained by the reduced phosphorylation of the initiation factor eIF4E and downregulation of the antiapoptotic protein Mcl-1 [25]. Sorafenib blocks the VEGFR-2 receptor, an effect which could be linked to anti-angiogenesis through decreased endothelial cell survival. Endothelial cell survival is assured through anti-apoptotic signalling, which normally occurs through Akt/PBK via the PI3 kinase-dependent pathway and up-regulation of anti-apoptotic protein signalling [26]. In support of this, sorafenib did decrease the phosphorylation of AKT in endothelial cells *in vitro* (data not shown).

The molecular mechanism by which everolimus and sorafenib combine to exert effective anti-tumor activity in MH-3924A derived tumors has been partly elucidated in our studies. The combination therapy did increase the pAkt Ser473/Akt ratio in our tumor model (Figures 5C and S3), which was likely due to the mTOR complex 2-dependent phosphorylation of Akt in tumoral cells. However, a higher AKT phosphorylation is not necessarily incompatible with a reduction in tumor growth [27], [28]. In fact, induction of p-AKT secondary to mTOR

inhibition was shown to be independent of the anti-proliferation cellular response to everolimus and modulation of AKT phosphorylation alone does not predict effects on downstream signalling [28]. Therefore, the anti-tumoral benefit of the combined treatment in our tumor model depends on pathways unrelated to the tumoral AKT signalling. The combination of everolimus and sorafenib also annulled the hypophosphorylation of 4E-BP1 elicited by everolimus alone in tumor tissue (Figure S3). However, the phosphorylation of the ribosomal protein S6 was completely inhibited in tumors treated with both everolimus and the combination (data not shown), which confirms the pharmacological inhibition of the mTOR complex 1. Since the MH-3924A cell line is insensitive to everolimus, and inhibition of S6 kinase and hypophosphorylated 4E-BP1 has been demonstrated in cell lines that were both sensitive and resistant to everolimus [28], we conclude that the ratio p4E-BP1/4E-BP1 in total tumoral tissue is not an adequate pharmacodynamic marker for the anti-tumoral effects of combined everolimus and sorafenib. The addition of everolimus to sorafenib annulled the effect of sorafenib on the phosphorylation of Erk1/2 and downstream pElk1 (Figure S3). One explanation is that Erk1/2 may be phosphorylated by a kinase other than Raf. A second explanation is that the phosphorylation of Erk1/2 could be regulated by cross talk between PI3K/Akt and MAPK signaling due to a feedback loop affecting the S6K-PI3K-Ras pathway [29]. The increase in ERK phosphorylation observed after the combined everolimus and sorafenib is not incompatible with better anti-tumoral properties because of the likelihood that MEK/ERK-independent mechanisms are responsible for the reduced growth of MH-3924A tumors. We argue that everolimus and sorafenib together reduced tumor growth *in vivo* more effectively than monotherapies primarily because of the combined effects of inhibition of mTOR signalling in endothelial cells and perhaps in non-tumor pericytes [20], and of sorafenib-induced tumor cell apoptosis and reduced anti-apoptotic signalling in endothelial cells and perhaps in other supportive cells of the vasculature.

A comparison of the peripheral tumor regions revealed distinct histological differences between treatment and control groups. The tumor front, which was linear and often encapsulated in the control group, appeared irregular and invasive after treatment, and prominently intermingled with the surrounding tissue to produce isolated islands of tumor tissue. These features were particularly evident in the combination group. Although this suggested a more invasive tumor phenotype [30], no distant metastases were detected in any of the animals at the time of harvesting. We speculate that the treated tumors differed from the untreated tumors because the treated tumors have evolved in an anti-angiogenic environment and must rely on the blood supply at the peripheral edges to support growth. Whether the differences in staining pattern of E-cadherin at the tumor interface influence the pattern of invasiveness observed is not known at this point [31].

Despite a superior reduction in tumor growth, the effect of the everolimus-sorafenib combination on the median survival remained modest in comparison to the other treatment options. Our survival study was designed with conditions wherein rats were euthanized when explicit endpoint criteria linked to distress had been reached. Because the endpoint criteria would have precipitated termination of the study for the distressed animals, the effect of the combination everolimus-sorafenib on the median survival was modest. We would expect a larger clinical effect on the median natural survival of patients.

The sequential administration of everolimus after sorafenib may be clinically useful in certain circumstances. In clinical trials, 40% of the HCC patients treated with sorafenib develop side effects severe enough to warrant discontinuation of the treatment. Such patients deprived of targeted therapy are then exposed to a rebound effect, which has been shown experimentally,

although no mechanism was postulated [32]. This rebound effect could be provoked partly by an increased concentration of growth factors such as VEGF as we report here, which may fuel tumor growth if left unopposed. Our results offer reassurance that patients can still benefit from an alternative systemic targeted therapy after sorafenib and that everolimus can still exert its antiangiogenic effects. However, the extent of the clinical improvement that can be offered to patients remains to be verified. One must also carefully consider whether the combination of an inhibitor of mTOR and sorafenib will be tolerated by patients with liver cirrhosis.

In conclusion, our results present mechanistic insights into the treatment of HCC with everolimus either in combination with sorafenib or in subsequent treatment and provide the experimental basis for testing this combination in clinical trials.

**ACKNOWLEDGMENTS:**

We thank Bayer for providing sorafenib and Novartis for providing everolimus. We thank M. Lederman for outstanding technical support and Dr. David Semela, University of Basel for providing the human hepatic sinusoidal endothelial cells. ACP is recipient of a grant from 'Cancer et Solidarité' and is supported by the ISJR Program. JFD is recipient of grants from Swiss National Foundation, Oncosuisse and the Sassella Stiftung.

**REFERENCES**


1. Llovet JM, Ricci S, Mazzaferro V, Hilgard P, Gane E, Blanc JF et al. Sorafenib in advanced hepatocellular carcinoma. N Engl J Med 2008;359:378-390.
2. Cheng AL, Kang YK, Chen Z, Tsao CJ, Qin S, Kim JS et al. Efficacy and safety of sorafenib in patients in the Asia-Pacific region with advanced hepatocellular carcinoma: a phase III randomised, double-blind, placebo-controlled trial. Lancet Oncol 2009;10:25-34.
3. Calvisi DF, Ladu S, Gorden A, Farina M, Conner EA, Lee JS et al. Ubiquitous activation of Ras and Jak/Stat pathways in human HCC. Gastroenterology 2006;130:1117-1128.
4. Wilhelm SM, Carter C, Tang L, Wilkie D, McNabola A, Rong H et al. BAY 43-9006 exhibits broad spectrum oral antitumor activity and targets the RAF/MEK/ERK pathway and receptor tyrosine kinases involved in tumor progression and angiogenesis. Cancer Res 2004;64:7099-7109.
5. Whittaker S, Marais R, Zhu AX. The role of signaling pathways in the development and treatment of hepatocellular carcinoma. Oncogene 2010;29:4989-5005.
6. Semela D, Piguet AC, Kolev M, Schmitter K, Hlushchuk R, Djonov V et al. Vascular remodeling and antitumoral effects of mTOR inhibition in a rat model of hepatocellular carcinoma. J Hepatol 2007;46:840-848.
7. Huynh H, Ngo VC, Koong HN, Poon D, Choo SP, Thng CH et al. Sorafenib and rapamycin induce growth suppression in mouse models of hepatocellular carcinoma. J Cell Mol Med 2009;13:2673-2683.
8. Yang R, Rescorla FJ, Reilly CR, Faught PR, Sanghvi NT, Lumeng L et al. A reproducible rat liver cancer model for experimental therapy: introducing a technique of intrahepatic tumor implantation. J Surg Res 1992;52:193-198.

9. Djonov VG, Kurz H, Burri PH. Optimality in the developing vascular system: branching remodeling by means of intussusception as an efficient adaptation mechanism. Dev Dyn 2002;224:391-402.

10. Lowry O, Rosebrough N, Farr L, Randall R. Protein measurement with the folin phenol reagent. J Biol Chem 1951;193:265-275.

11. Sieghart W, Fuereder T, Schmid K, Cejka D, Werzowa J, Wrba F et al. Mammalian target of rapamycin pathway activity in hepatocellular carcinomas of patients undergoing liver transplantation. Transplantation 2007;83:425-432.

12. Villanueva A, Chiang DY, Newell P, Peix J, Thung S, Alsinet C et al. Pivotal role of mTOR signaling in hepatocellular carcinoma. Gastroenterology 2008;135:1972-1983, 1983 e1971-1911.

13. Boyault S, Rickman DS, de Reynies A, Balabaud C, Rebouissou S, Jeannot E et al. Transcriptome classification of HCC is related to gene alterations and to new therapeutic targets. Hepatology 2007;45:42-52.

14. Newell P, Toffanin S, Villanueva A, Chiang DY, Minguez B, Cabellos L et al. Ras pathway activation in hepatocellular carcinoma and anti-tumoral effect of combined sorafenib and rapamycin in vivo. J Hepatol 2009;51:725-733.

15. Wang Z, Zhou J, Fan J, Qiu SJ, Yu Y, Huang XW et al. Effect of rapamycin alone and in combination with sorafenib in an orthotopic model of human hepatocellular carcinoma. Clin Cancer Res 2008;14:5124-5130.

16. Semela D, Dufour JF. Angiogenesis and hepatocellular carcinoma. J Hepatol 2004;41:864-880.

17. Drevs J. Soluble markers for the detection of hypoxia under antiangiogenic treatment. Anticancer Res 2003;23:1159-1161.

18. Zhu AX, Sahani DV, Duda DG, di Tomaso E, Ancukiewicz M, Catalano OA et al. Efficacy, safety, and potential biomarkers of sunitinib monotherapy in advanced hepatocellular carcinoma: a phase II study. J Clin Oncol 2009;27:3027-3035.

19. Saranadasa M, Wang ES. Vascular endothelial growth factor inhibition: Conflicting roles in tumor growth. Cytokine 2010.

20. Lane HA, Wood JM, McSheehy PM, Allegrini PR, Boulay A, Brueggen J et al. mTOR inhibitor RAD001 (everolimus) has antiangiogenic/vascular properties distinct from a VEGFR tyrosine kinase inhibitor. Clin Cancer Res 2009;15:1612-1622.

21. O'Reilly T, McSheehy PM. Biomarker Development for the Clinical Activity of the mTOR Inhibitor Everolimus (RAD001): Processes, Limitations, and Further Proposals. Transl Oncol 2010;3:65-79.

22. Di Nicolantonio F, Arena S, Tabernero J, Grosso S, Molinari F, Macarulla T et al. Deregulation of the PI3K and KRAS signaling pathways in human cancer cells determines their response to everolimus. J Clin Invest;120:2858-2866.

23. Hosoi H, Dilling MB, Liu LN, Danks MK, Shikata T, Sekulic A et al. Studies on the mechanism of resistance to rapamycin in human cancer cells. Mol Pharmacol 1998;54:815-824.

24. Cote GJ, Lastra BA, Cook JR, Huang DP, Chiu JF. Oncogene expression in rat hepatomas and during hepatocarcinogenesis. Cancer Lett 1985;26:121-127.

25. Wilhelm SM, Adnane L, Newell P, Villanueva A, Llovet JM, Lynch M. Preclinical overview of sorafenib, a multikinase inhibitor that targets both Raf and VEGF and PDGF receptor tyrosine kinase signaling. Mol Cancer Ther 2008;7:3129-3140.

26. Gerber HP, McMurtrey A, Kowalski J, Yan M, Keyt BA, Dixit V et al. Vascular endothelial growth factor regulates endothelial cell survival through the

phosphatidylinositol 3'-kinase/Akt signal transduction pathway. Requirement for Flk-1/KDR activation. J Biol Chem 1998;273:30336-30343.

27. Fuereder T, Jaeger-Lansky A, Hoeflmayer D, Preusser M, Strommer S, Cejka D et al. mTOR inhibition by everolimus counteracts VEGF induction by sunitinib and improves anti-tumor activity against gastric cancer in vivo. Cancer Lett;296:249-256.

28. Breuleux M, Klopfenstein M, Stephan C, Doughty CA, Barys L, Maira SM et al. Increased AKT S473 phosphorylation after mTORC1 inhibition is rictor dependent and does not predict tumor cell response to PI3K/mTOR inhibition. Mol Cancer Ther 2009;8:742-753.

29. Carracedo A, Ma L, Teruya-Feldstein J, Rojo F, Salmena L, Alimonti A et al. Inhibition of mTORC1 leads to MAPK pathway activation through a PI3K-dependent feedback loop in human cancer. J Clin Invest 2008;118:3065-3074.

30. Paez-Ribes M, Allen E, Hudock J, Takeda T, Okuyama H, Vinals F et al. Antiangiogenic therapy elicits malignant progression of tumors to increased local invasion and distant metastasis. Cancer Cell 2009;15:220-231.

31. Moon KC, Cho SY, Lee HS, Jeon YK, Chung JH, Jung KC et al. Distinct expression patterns of E-cadherin and beta-catenin in signet ring cell carcinoma components of primary pulmonary adenocarcinoma. Arch Pathol Lab Med 2006;130:1320-1325.

32. Ebos JM, Lee CR, Cruz-Munoz W, Bjarnason GA, Christensen JG, Kerbel RS. Accelerated metastasis after short-term treatment with a potent inhibitor of tumor angiogenesis. Cancer Cell 2009;15:232-239.

**FIGURE LEGENDS**

**Fig. 1. Effect of the combination of everolimus and sorafenib on tumor growth and survival of rats implanted with Morris Hepatoma tumor cells. A. Representative magnetic resonance images (MRI) of the liver of untreated (vehicle) and treated rats.** MRI images were generated 35 days after tumor cell implantation. The tumors (arrows) are smaller in each treatment group than in the untreated liver. **B. Tumor volume as a function of time in untreated and treated rats.** The volume of tumors was measured on MRI images taken weekly after tumor cell implantation. On day 35, when compared to untreated tumors, the tumor volumes had decreased by 29% after sorafenib treatment, 55% after sequential sorafenib then everolimus, 50% after everolimus and 85% after combined treatment. (*, $p<0.01$ in comparison to control; +, $p<0.01$ in comparison to combination; #, $p<0.05$ in comparison to sorafenib; N=6 for control, everolimus and sequential treatments, N=5 for sorafenib treatment and N=4 combination treatment). **C. Survival curve of rats implanted with MH tumor cells.** The median survival was 57 days in the control group, 63.5 days when treated with sorafenib and 70 days when treated with the combination sorafenib-everolimus (*, $p<0.001$ vs vehicle, +, $p<0.001$ vs sorafenib; N=7 for vehicle treatment, N=6 for sorafenib treatment and N=5 for combination treatment).

**Fig. 2. Effect of the combination of everolimus and sorafenib on tumor necrosis (A), tumor apoptosis (B and C) and tumor hypoxia (D). A. Extent of necrosis, assessed by Giemsa staining, in tumors of rats implanted with Morris Hepatoma cells.** The percentage of necrotic area relative to the total area was quantified. The necrotic area was similar in all groups although necrosis was slightly but not significantly increased in the combination group (N=6 for vehicle and sequential treatments, N=5 for everolimus and sorafenib treatments and N=4 for combination treatment). **B. and C. Apoptosis in tumoral**

**tissue assessed by the presence of cleaved-caspase 3**. Immunoblots **(B)** of cleaved caspase-3 were compared in liver tumors from rats untreated (vehicle) and treated with everolimus and sorafenib, alone or in combination. Two to three representative immunoblots from each treatment group are shown. Actin was used as a loading control. Immunostaining (**C, 10x magnification**) for cleaved caspse-3 in tumors representating untreated (vehicle) and treated groups. Compared to the untreated group, the amount of cleaved-caspase 3 tended to increase in tumors of animals treated with everolimus, sorafenib, the combination of both drugs or with the sequential treatment. **D. Hypoxia of liver tumors assessed by HIF-1α immunostaining (10x magnification).** Compared to the untreated group, the number of HIF-1α positive cells was significantly increased by everolimus, sorafenib, the combination of drugs and the sequential treatment.

**Fig. 3. Effect of the combination of everolimus and sorafenib on rat aortic endothelial cell and Morris Hepatoma cell proliferation. A.** Cell proliferation was measured by $^{3}$H-Thymidine incorporation into rat aortic endothelial cells. Sorafenib did not affect proliferation of aortic endothelial cells. Everolimus 20nM significantly decreased proliferation by 40%. There was no additive effect when sorafenib and everolimus were combined. (*, $p<0.05$ vs complete medium). **B.** In Morris Hepatoma cells, sorafenib 10μM inhibited the proliferation, in contrast to everolimus. The minimum effective concentration of sorafenib was lowered to 5μM upon the addition of everolimus. Experiments were performed three times in triplicate; *, $p<0.05$ vs complete medium, #, $p<0.05$ vs sorafenib 5μM, +, $p<0.05$ vs sorafenib 10μM and $, $p<0.05$ vs everolimus 20nM + sorafenib 10μM.

**Fig. 4. Effect of the combination of everolimus and sorafenib on angiogenesis in vitro. A.** Aortic rings isolated from ACI rats were incubated in medium on Matrigel with or without

everolimus 200nM and/or sorafenib 100nM. After 5 days of incubation, rings were fixed, stained and photographed (left). Vascular outgrowth was quantified by counting all capillary sprouts from one ring and normalizing to vehicle (control) (right). Both everolimus and sorafenib alone significantly decreased vessel sprouting compared to the vehicle group. This effect was greater when the drugs were combined and further magnified when rings were incubated with sorafenib for 2 days then everolimus (N=6 for each experimental condition) (*, $p<0.05$ vs vehicle, +, $p<0.05$ vs sorafenib 100nM, then everolimus 200nM). **B.** Human hepatic sinusoidal endothelial cells were incubated on Matrigel with or without everolimus 20nM and/or sorafenib 100nM. After 72 hours of incubation, photomicrographs were recorded at random. Areas covered by vascular tubes were digitally quantified using the software Metamorph. Everolimus significantly decreased capillary tube formation, compared to the vehicle group. Addition of sorafenib did not further increase this effect (*, $p<0.05$ vs vehicle.

**Fig. 5. Effect of everolimus and sorafenib treatment on gene expression of *Vegf-a* and on the phosphorylation of target proteins in tumoral tissue. A. Tumoral mRNA expression of *Vegf-a*.** mRNA was extracted from liver tumors and the level of *Vegf-a* was measured by quantitative real-time PCR. Compared to the vehicle (control) group, *Vegf-a* mRNA increased after sorafenib (*, $p<0.05$ vs vehicle). Tumors treated with the combination of everolimus and sorafenib expressed higher mRNA levels of *Vegf-a* than everolimus alone ( +, $p<0.05$ vs everolimus). N=6 for sequential treatment, N=5 for vehicle and everolimus treatments, N=4 for sorafenib and combination treatment. **B. Effect of treatment on the expression and phosphorylation of 4E-BP1 and Erk1/2 in tumors.** Immunoblots of phosphorylated 4E-BP1 and Erk1/2, which are target proteins of everolimus and sorafenib, respectively, were quantified. The membranes were then stripped and reprobed with

antibodies against 4E-BP1 and Erk1/2 to measure total levels of each protein. Actin was used as a loading control. The immunoblots shown are representative of each group. **C. Effect of treatment on the phosphorylation of Akt (Ser473) in tumoral tissue**. The phosphorylation of Akt (Ser473) was assessed by immunoblotting. The membrane was then stripped and reprobed with antibodies against Akt to measure the total level of the protein. Actin was used as a loading control. The immunoblots shown are representative of results from each group

**Fig. 6. Effect of everolimus and sorafenib on the vascular morphology and on the tumoral periphery. A. Effect of sorafenib and combined sorafenib-everolimus on the vascular morphology of the tumors using the vascular casts technique.** The SEM microphotograph shows a typical tumoral vascular pattern with abundant vascular sprouts (arrows) in the untreated (vehicle) tumor (left panel). In the sorafenib-treated tumor (middle panel), the vascular sprouts are rare (arrows) whereas pillars (arrowheads) are a frequent finding. In the group treated with everolimus and sorafenib (right panel), vascular sprouts were absent and the larger sinusoidal vessels were pierced with numerous, irregularly positioned pillars (arrowheads). Bars measure 20 μM for vehicle and sorafenib sections and 10 μM for everolimus+sorafenib. **B.** Histological analysis of the periphery of untreated and treated hepatic tumors. The periphery of untreated (drug vehicle) tumors was regular, encircled by a limiting capsule and showed no vascular invasion (left). Tumors treated with a combination of sorafenib and everolimus show an invasive front at the periphery, which extensively intercalates into the surrounding tissue (right).

**Figure 1**

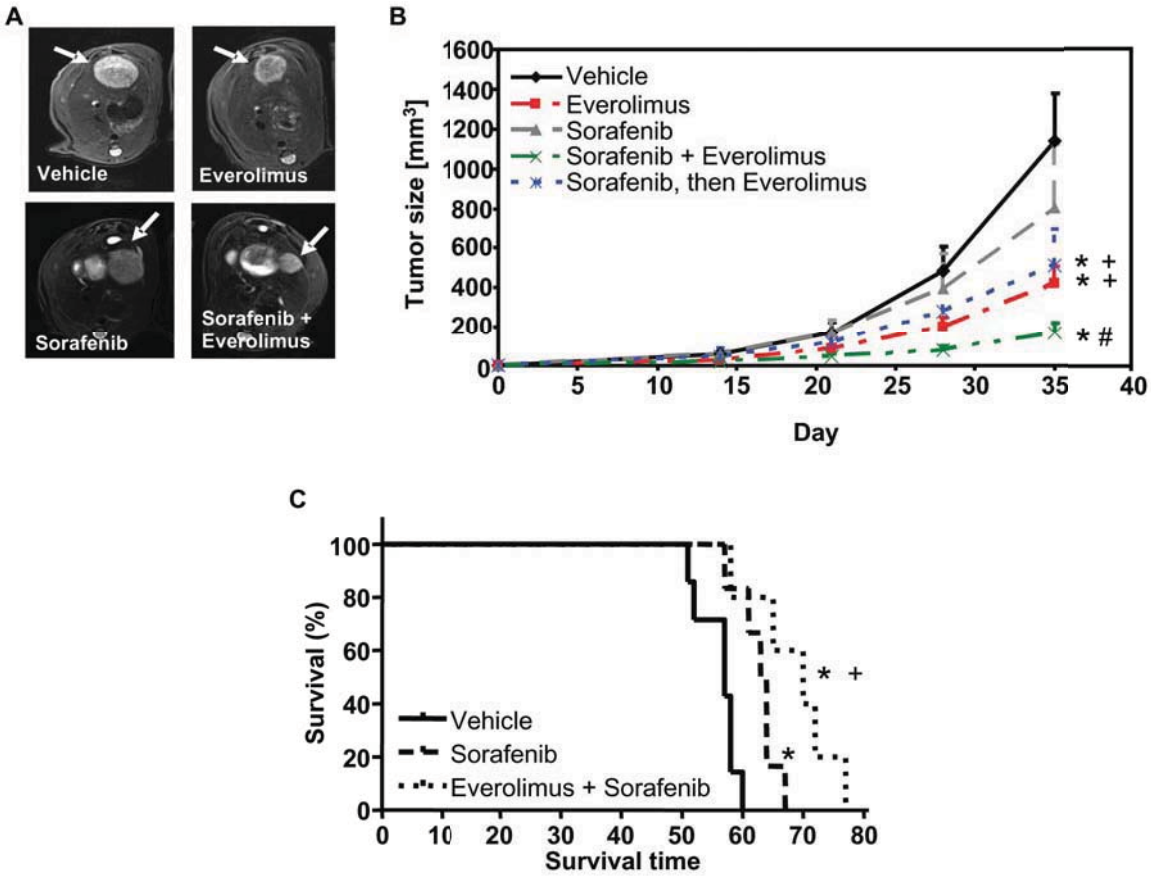

**Figure 2**

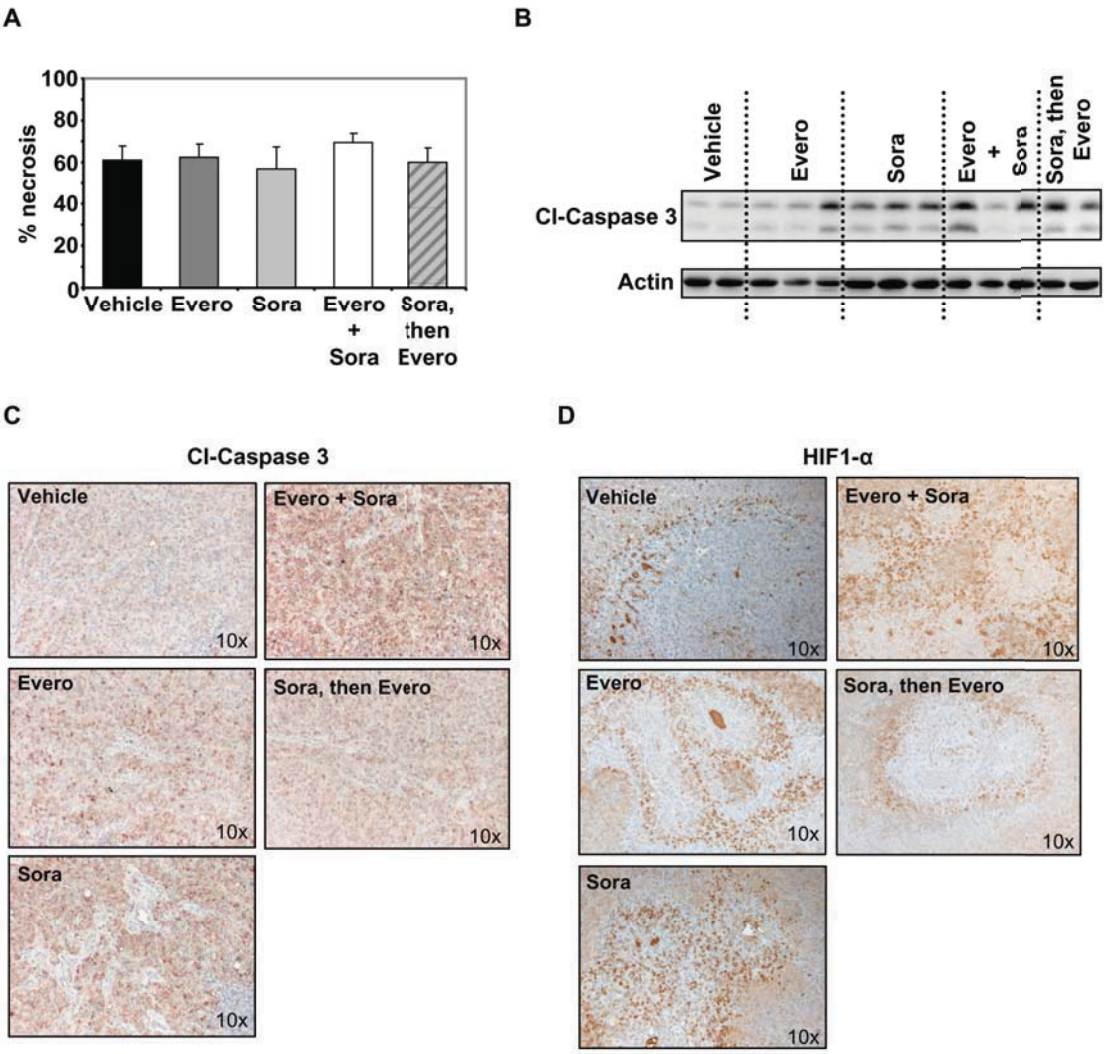

**Figure 3**

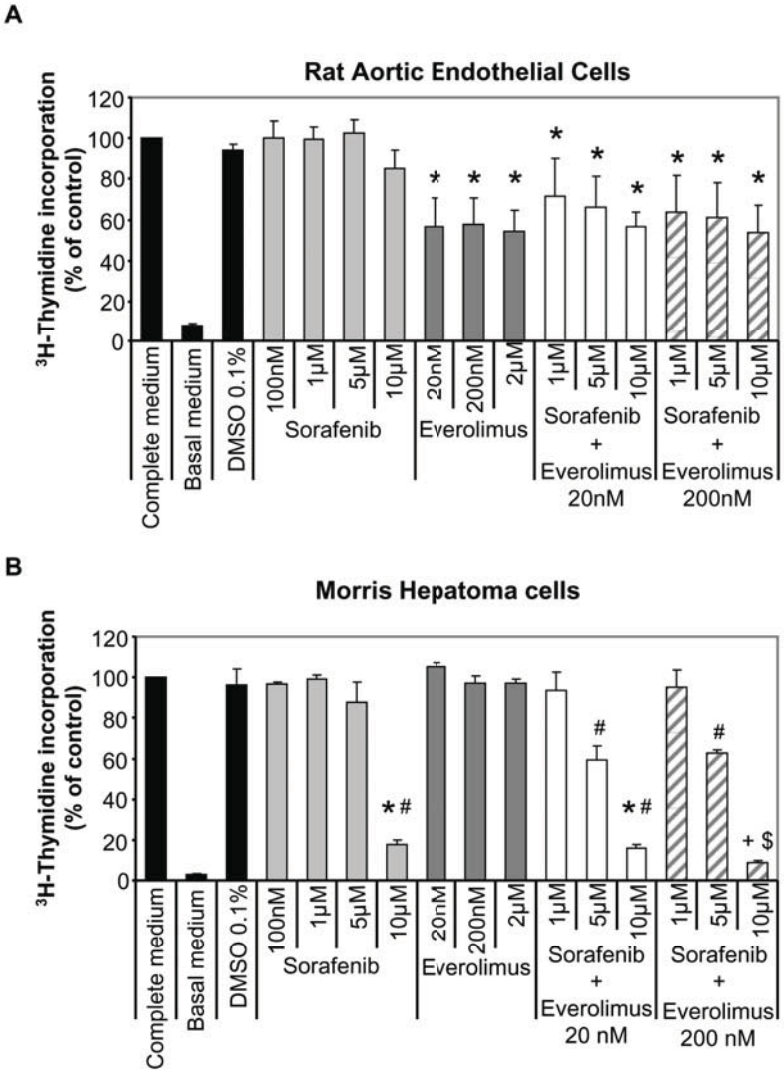

**Figure 4**

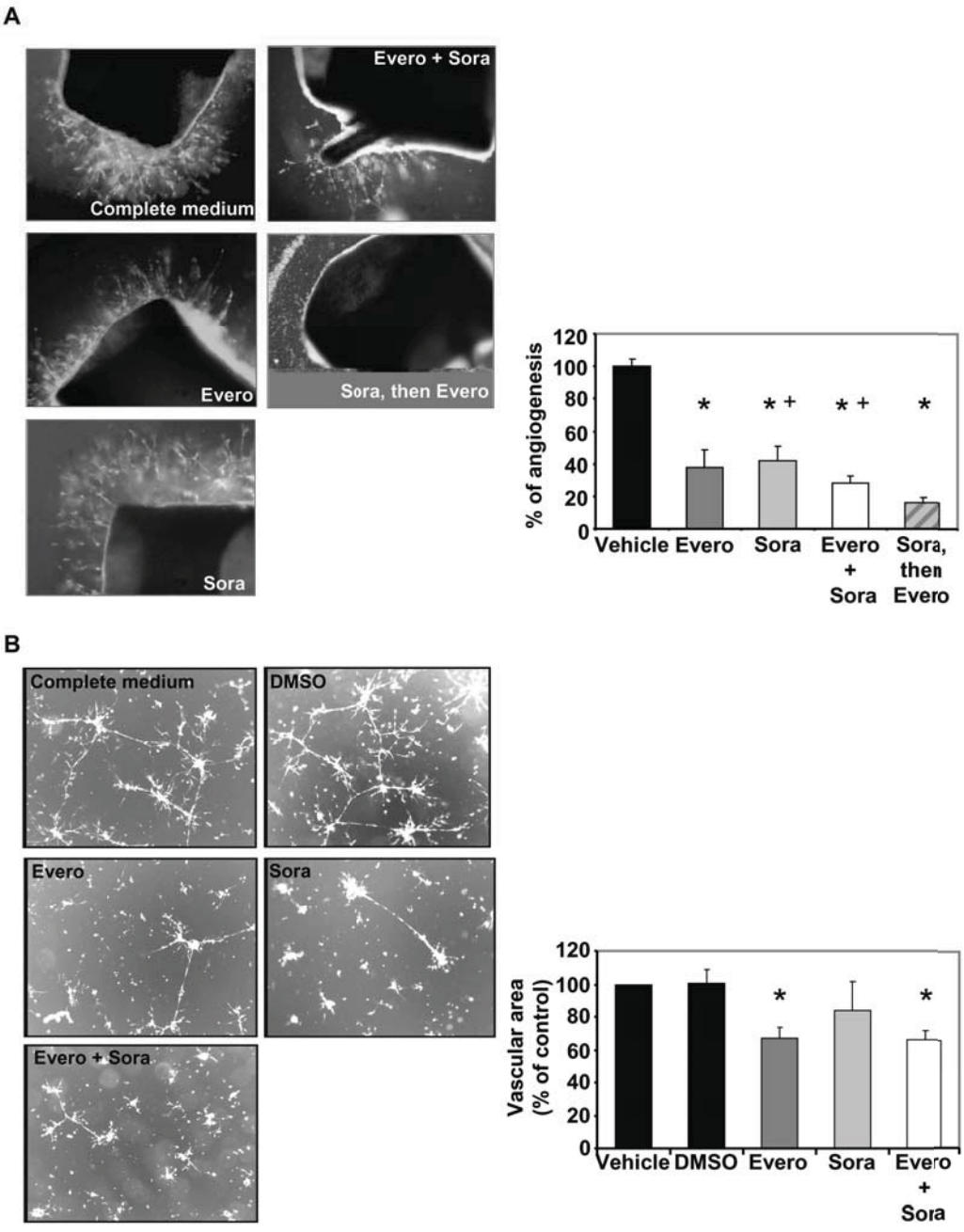

**Figure 5**

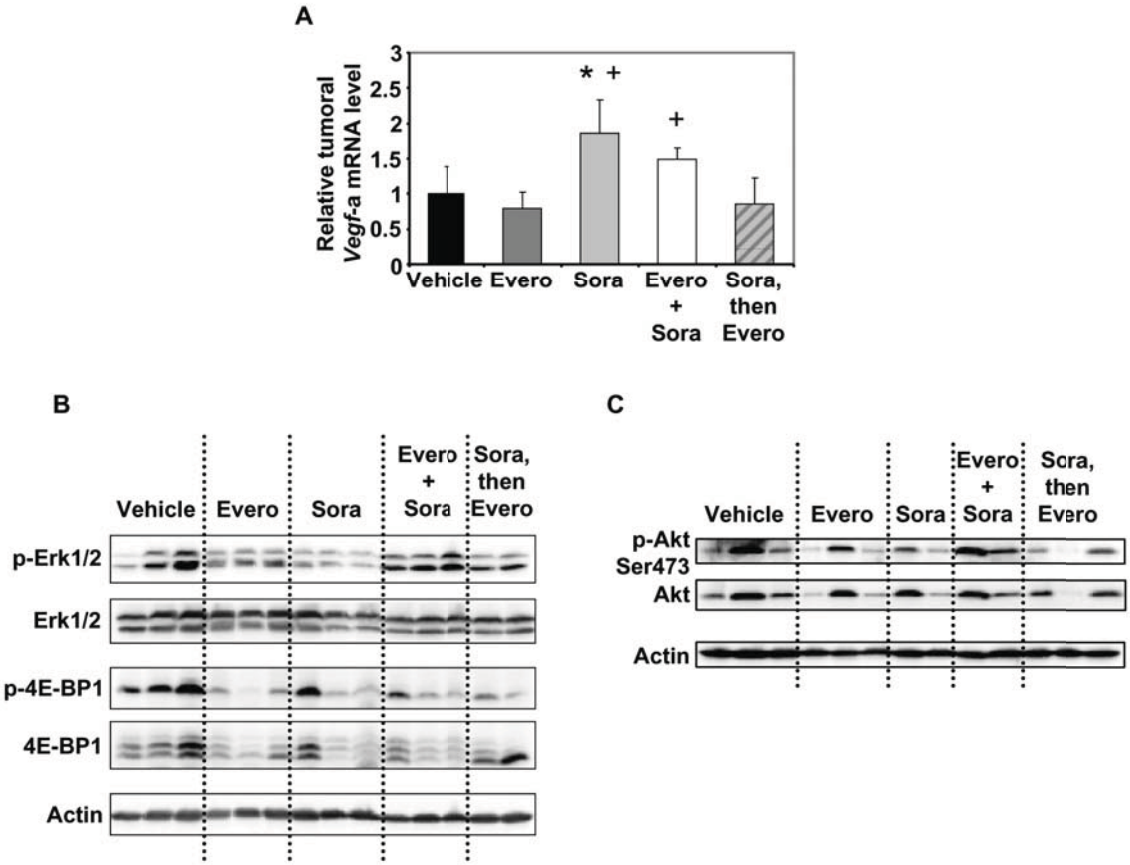

**Figure 6**